EFDA–JET–PR(07)21

T. Tala, K. Crombé, P.C. de Vries, J. Ferreira, P. Mantica, A.G. Peeters, Y. Andrew, R. Budny, G. Corrigan, A. Eriksson, X. Garbet, C. Giroud, M.-D. Hua, H. Nordman, V. Naulin, M.F.F. Nave, V. Parail, K. Rantamäki, B.D. Scott, P. Strand, G. Tardini, A. Thyagaraja, J. Weiland, K.-D. Zastrow and JET-EFDA contributors

Toroidal and Poloidal Momentum Transport Studies in Tokamaks

Toroidal and Poloidal Momentum Transport Studies in Tokamaks

T. Tala[1], K. Crombé[2], P.C. de Vries[3], J. Ferreira[4], P. Mantica[5], A.G. Peeters[6], Y. Andrew[3], R. Budny[7], G. Corrigan[3], A. Eriksson[8], X. Garbet[9], C. Giroud[3], M.-D. Hua[3], H. Nordman[8], V. Naulin[10], M.F.F. Nave[4], V. Parail[3], K. Rantamäki[1], B.D. Scott[11], P. Strand[8], G. Tardini[11], A. Thyagaraja[3], J. Weiland[8], K.-D. Zastrow[3]
and JET-EFDA contributors*

JET-EFDA, Culham Science Centre, OX14 3DB, Abingdon, UK

[1]*Association EURATOM-Tekes, VTT, P.O. Box 1000, FIN-02044 VTT, Finland*
[2]*Department of Applied Physics, Ghent University, Belgium*
[3]*EURATOM/UKAEA Fusion Association, Culham Science Centre, Oxon. OX14 3DB, UK*
[4]*Associação EURATOM/IST, Centro de Fusão Nuclear, 1049-001 Lisbon, Portugal*
[5]*Istituto di Fisica del Plasma CNR-EURATOM, via Cozzi 53, 20125 Milano, Italy*
[6]*Center for Fusion, Space and Astrophysics, Department of Physics, University of Warwick, CV4 7AL, UK*
[7]*Princeton Plasma Physics Laboratory, New Jersey, USA*
[8]*Association EURATOM-VR, Chalmers University of Technology, Göteborg, Sweden*
[9]*Association EURATOM-CEA, CEA/DSM/DRFC Cadarache, St Paul-Lez-Durance, France*
[10]*Association Euratom-Risø National Laboratory, Technical University od Denmark, DK-4000 Roskilde, Denmark*
** See annex of M.L. Watkins et al, "Overview of JET Results", (Proc. 21st IAEA Fusion Energy Conference, Chengdu, China (2006)).*

Preprint of Paper to be submitted for publication in
Plasma Physics and Controlled Fusion

ABSTRACT.
This paper reports on recent studies of toroidal and poloidal†momentum transport†in tokamaks. The ratio of the global energy confinement time to the momentum confinement is found to be close to $t_E/t_f = 1$ among several tokamaks. On the other hand, local transport analysis in the core plasma shows a larger scatter in the ratio of the local effective momentum diffusivity to the ion heat diffusivity $\chi_{\phi,eff}/\chi_{i,eff}$ among different tokamaks, for example the value of effective Prandtl number being typically around $\chi_{\phi,eff}/\chi_{i,eff} \approx 0.2$ on JET. Perturbative NBI modulation experiments on JET have shown, however, that a Prandtl number χ_ϕ/χ_i of around 1 is valid if there is an additional, significant inward momentum pinch which is required to explain the amplitude and phase behaviour of the momentum perturbation. The experimental results, i.e. the high Prandtl number and pinch, are in good qualitative and to some extent also in quantitative agreement with linear gyro-kinetic simulations. Concerning the poloidal velocity, the experimental measurements on JET show that the carbon poloidal velocity can be an order of magnitude above the neo-classical estimate within the ITB. This significantly affects the calculated radial electric field and therefore, the $E\times B$ flow shear used for example in transport simulations. Several fluid turbulence codes have been used to identify the mechanism driving the poloidal velocity to such high values. CUTIE and TRB turbulence codes and also the Weiland model predict the existence of an anomalous poloidal velocity, peaking in the vicinity of the ITB and being dominantly caused by flow due to the Reynold's stress. It is important to note that both codes treat the equilibrium in a simplified way and this affects the geodesic curvature effects and Geodesic Acoustic Modes (GAMs). The neo-classical equilibrium is calculated more accurately in the GEM code and the simulations suggest that the spin-up of poloidal velocity is a consequence of the plasma profiles steepening when the ITB grows, following in particular the growth of the toroidal velocity within the ITB.

1. INTRODUCTION

Of all the transport channels relevant to a tokamak, the transport of momentum is the least well studied or understood. The plasma rotation is of interest, however, since a sheared rotation can lead to the quenching of turbulence [1, 2, 3] and, hence, an improvement in confinement. Such an improvement can be both moderate as well as dramatic through the formation of a transport barrier. For the latter phenomenon experiments indicate that the toroidal and in particular the poloidal velocity play an important role in the dynamics of ITBs. In addition, toroidal rotation gives stability against beta-limiting resistive wall modes by making the stationary wall more conducting [4, 5, 6, 7].

For these reasons the study of momentum transport is currently an active area of research, both theoretically as well as experimentally. Recent experiments have yielded a Prandtl number (ratio of the effective momentum diffusivity and the effective ion heat conductivity coefficients, see below) substantially below one [8, 9, 10] in apparent contradiction with the gyro-kinetic calculations [11, 12]. New developments in the theory, however, suggest that this discrepancy could possibly be resolved through the existence of a momentum pinch velocity [13]. Experiments in which the poloidal rotation

at the onset of the internal transport barrier were measured yielded a rotation far larger than predicted by neoclassical theory [14, 15, 16], which again present a challenge for theoretical modelling.

From the radial force balance equation for E_r, the $E\times B$ flow shearing rate $\omega_{E\times B}$ [17] can be written as follows:

$$E_r = \frac{1}{eZ_i n_i}\frac{\partial p_i}{\partial r} - v_{\theta,i} B_\phi + v_{\phi,i} B_\theta, \qquad \omega_{E\times B} = \frac{r}{q}\frac{\partial\left(q v_E / r\right)}{\partial r} \tag{1}$$

where Z_i is the charge number, n_i the density, p_i the pressure, $v_{\theta,i}$ the poloidal velocity and $v_{\phi,i}$ the toroidal velocity of the ion species i, v_E is the $E\times B$ velocity, q is the safety factor and B_ϕ and B_θ are toroidal and poloidal components of the magnetic field.

This paper reports on recent experimental and modelling studies of both toroidal and poloidal momentum transport in tokamaks. The main issues around which the paper is focused are 1) the relation of heat and momentum transport in tokamaks, 2) question on whether the theoretically predicted momentum pinch can be verified experimentally, 3) can the toroidal rotation profile in ITER be predicted reliably and 4) the relation of the poloidal velocity to transport barrier onset and dynamics and driving mechanisms of poloidal velocity against the neoclassical viscous damping.

2.COMPARISON OF TOROIDAL MOMENTUM AND ION HEAT TRANSPORT

It has been reported in several large tokamaks that the toroidal momentum confinement time τ_ϕ is very similar to the energy confinement time τ_E [18,19,20,21,22]. This similarity $\tau_E/\tau_\phi \sim 1$ has been further confirmed recently on JET using the momentum transport database consisting of several hundreds of discharges [8]. τ_ϕ and τ_E are defined as the total momentum content divided by the torque and total energy content divided by the total heating power during the steady-state phase of the discharge, respectively. Here the torque is equal to the torque from the Neutral Beam Injection (NBI) even if it is known that there are other sources of rotation and torque than the NBI. The role of intrinsic rotation has been reported on many tokamaks in several papers [23,24,25]. The magnitude of intrinsic or Ion Cyclotron Resonance Heating (ICRH) induced toroidal rotation was also reported recently in JET Ohmic and in ICRF heated plasmas [26, 27], finding that the magnitude of intrinsic rotation in JET Ohmic plasmas (LHCD only) is an order of magnitude smaller (typically 3-10%) than in dominantly NBI heated plasmas. Also in references [26, 27], the intrinsic rotation on JET has been found to scale with plasma current and diamagnetic energy, the rotation velocities, however, being always about 10% of those in strongly NBI heated plasmas. A scaling law for intrinsic plasma rotation with plasma β has been recently proposed†in reference [28], but in JET, it is very difficult to have high β plasmas without significant NBI heating to confirm the scaling. As a consequence of the recent results on magnitude of intrinsic rotation on JET, in this paper we can rather safely restrict ourselves to momentum transport studies in plasmas where the NBI torque is the dominant source of momentum and other sources of torque can be neglected. It should be also noted that studies of the global confinement times include the edge pedestal, and in many cases a significant

fraction of the confinement comes from the edge. However, in this paper we concentrate on momentum transport studies in the plasma core.

Based on the results from studies of global momentum and energy confinement, one could expect to have very similar momentum and ion heat diffusivities in tokamaks. However, although the global momentum and energy confinement times would be the same, the local diffusivities in the core plasma may well be different, in particular because the edge momentum pedestal is often weaker although the knowledge of local momentum transport within the pedestal is rather limited. On the other hand, equal diffusivities $P_r = \chi_\phi/\chi_i=1$ in the plasma core were predicted long time ago in the early days of the ITG theory [29]. This assumption has been also commonly used in ITER predictions.

Using the momentum database, it is possible to calculate the effective diffusivities and effective Prandtl number $P_r = \chi_{\phi,eff}/\chi_{i,eff}$ from

$$\chi_{\phi,eff} = \frac{\Gamma_\phi}{\nabla mnR\omega_\phi} \tag{2}$$

$$\chi_{i,\,eff} = \frac{q_i}{n\nabla T_i} \tag{3}$$

where q_i and Γ_ϕ are the heat and torque fluxes, ω_ϕ the angular frequency, T_i and n_i the ion temperature and density, and m and R are the mass and major radius, respectively. Here, the torque flux Γ_ϕ includes only the NBI driven torque, and therefore, the torque sources from intrinsic rotation and ICRF heating are neglected.

The ratio of effective momentum diffusivity to the ion heat diffusivity is shown in figure 1 for a large number of discharges from the JET momentum database, covering pulses from several different plasma scenarios. The values of the diffusivities are averaged over the gradient region at $r = 0.4–0.7$.

It is to note that the ratio $\chi_{\phi,eff}/\chi_{i,eff}$ on JET is significantly smaller than 1, the average value being around $\chi_{\phi,eff}/\chi_{i,eff} = 0.25$. Effective Prandtl numbers smaller than 1 have been also reported on ASDEX-Upgrade [10], although in the central part of the plasma inside r<0.5 values of $\chi_{\phi,eff}/\chi_{i,eff} = 1$ have been recently reported on ASDEX-Upgrade [30]. On the other hand, values around $\chi_{\phi,eff}/\chi_{i,eff} \approx 1$ have been reported on DIII-D [20], JT-60U [31] and TFTR [32]. There are two interesting observations concerning the effective Prandtl numbers; 1) the effective Prandtl numbers can be significantly below 1 and 2) there is quite a large scatter in the values among the different tokamaks.

There are at least two aspects that can affect both the trends in the global confinement times and the calculated ratio of local effective momentum diffusivity to the local effective ion heat diffusivity in the core plasma. The first one is the intrinsic rotation, but at least in JET with significant NBI heating directed in the co-current direction giving a large torque, the role of intrinsic rotation in the estimation of the effective Prandtl number through the additional torque in equation (2) is small. The second issue is the momentum pinch velocity. It has been predicted theoretically to be significant in recent papers [13, 33]. Dividing the momentum flux into the diffusive and pinch terms, one can write the effective diffusivity as

$$\chi_{\phi,eff} = \chi_{\phi}\left[1 + \frac{Rv_{pinch}}{\chi_{\phi}}\frac{1}{R/L_u}\right], \quad (4)$$

where χ_ϕ is the actual momentum diffusivity, v_{pinch} is the momentum pinch velocity (negative value inwards) and L_u is the gradient length of the normalised toroidal velocity ($u = v_\phi/v_{th}$=Mach number). The ratio Rv_{pinch}/χ_ϕ is defined as the pinch number. As can be seen in equation (4), the effective Prandtl number $\chi_{\phi,eff}/\chi_{i,eff}$ can be significantly different from the Prandtl number with diffusive terms only χ_ϕ/χ_i if the momentum pinch velocity is large. However, steady-state analysis does not allow to separate the relative weight of the diffusion and pinch terms in the momentum flux and therefore, transient momentum transport experiments are needed to study the momentum transport processes more deeply.

3. Perturbative Momentum Transport Experiments

An experiment where the NBI power and torque were modulated has been performed recently on JET with a modulation frequency of 6.25Hz. An H-mode plasma with type III ELMs at low collisionality and high q_{95} to avoid sawteeth was chosen to perform the cleanest possible rotation modulation. Active CX spectroscopy was used to measure the toroidal rotation ω_ϕ and T_i with a time resolution of 10 ms at 12 radial points. The modulation took place between t = 4s and t = 13s, and a zoom into the time interval between 8-10s is illustrated in figure 2, depicting the clear modulation in the NBI power, ion and electron temperatures and toroidal angular frequency ω_ϕ.

There are two different mechanisms responsible for how the torque deposition takes place. The first one is called collisional torque due to slowing down of fast beam injected on passing orbits ions colliding and exchanging their torque with thermal ions, producing a time delayed torque peaked dominantly on-axis, and the second one takes place due to beam ions injected into trapped orbits, which then generates an instantaneous $j\times B$ torque, peaked dominantly off-axis. Torque for the simulations shown in figure 2 has been calculated with the NUBEAM package inside the TRANSP transport code. Calculating the Fourier components of the modulated torque, one can see that the 1st harmonic (6.25Hz) of the modulation is affected by both the collisional and $j\times B$ components, whilst the 3rd harmonic, although much more noisy, is only determined by the $j\times B$ torque. However, as the modulated torque is not radially localised, determination of the momentum diffusivity and pinch is difficult directly from the data, but it is still possible indirectly with modelling.

The first step in the modelling aiming to determine the experimental momentum diffusivity and pinch is to choose the ion heat diffusion coefficient that reproduces the experimental steady-state temperature. The ion heat diffusivity «$_i$ in the simulations is chosen to match the experimental effective ion heat diffusivity $\chi_{i,eff}$ and this choice, inevitable reproduces the experimental T_i profile. After having fixed χ_i, several transport simulations with different combinations of Prandtl number χ_ϕ/χ_i and v_{pinch} are simulated in order to reproduce the steady-state ω_ϕ. Two of these options will be discussed in more detail. In the first one, the Prandtl number is fixed to $\chi_\phi/\chi_i = 0.25$ and $v_{pinch} = 0$ and in the

second one, χ_ϕ/χ_i = 1.0 and v_{pinch} = 15m/s (inwards and constant in radius). The first choice is motivated by the effective Prandtl number being around 0.25 for this pulse, which is a very typical value on JET plasmas as shown already in figure 1. Both these simulations predict the steady-state $\ldots_f$ within acceptable accuracy in the gradient region (not in the very centre inside r<0.2). However, it does not allow us to make any preference between the two choices of χ_ϕ/χ_i and v_{pinch} and therefore, the modelling is extended to cover the amplitude and phase of the Fourier harmonic of the perturbed momentum modulation as well. In all the transport simulations with the JETTO transport code [34], q-profile, T_e and n_e are frozen to their experimental values.

The experimental amplitudes and phases of the modulated ω_ϕ are compared in figure 3 with the simulated ones using the same two choices of momentum diffusivity and pinch. The left frame shows the simulation with χ_ϕ/χ_i = 0.25 and v_{pinch} = 0 and clearly, the disagreement with the experimental signals is striking. The simulated phase is too large everywhere, and this is an indication of too low momentum diffusivity or too low Prandlt number. In addition, the simulated amplitude is far too low towards the plasma centre, and this on the other hand is indicative of a need for an inward momentum pinch velocity (as the phase is already too large). Looking into the right frame, the simulation with χ_ϕ/χ_i = 1.0 and v_{pinch} = 15 m/s improves significantly the agreement with the experimental amplitude and phase. Using the choices χ_ϕ/χ_i in the range of 0.8–1.2 and v_{pinch} in the range of 8–15m/s all reproduce the experimental phase and amplitude roughly within the same acceptable accuracy, indicating the range of error bars in the analysis. In order to improve the accuracy, radially varying pinch velocities instead of the present radially constant pinch velocity profile should be used, as it is believed for example that the pinch decreases towards the plasma centre. In addition, the uniform pinch velocity does not fit very well the 3rd Fourier harmonic of the amplitude and phase that though quite noisy is above the noise level. These results yield the first experimental evidence of an inward momentum pinch on JET and also the evidence of a rather large Prandtl number χ_ϕ/χ_i. Recently also on JT-60U, torque modulation has been successfully exploited taking advantage of the lost ions due to toroidal field magnetic ripple at the plasma edge [31]. The momentum diffusivity and pinch could be directly evaluated there because the torque was locally modulated only at the edge. The results clearly showed that firstly, there is a significant inward momentum pinch and secondly, the Prandtl number is around 1.

4 MODELLING OF MOMENTUM TRANSPORT AND COMPARISON WITH THE EXPERIMENT

In this section, both the gyro-kinetic and fluid transport model simulations are compared with experimental data. The linear gyro-kinetic simulations with the LINART code [35] predict in general the Prandtl number around χ_ϕ/χ_i = 0.7–1 and a significant inward momentum pinch velocity [13]. The Prandtl number is also found to be rather independent of the plasma parameters and profiles, such as q, magnetic shear, gradient lengths etc. and does not largely change with kinetic electron effects compared with the adiabatic electron assumption [12]. On the hand, the pinch velocity has

a stronger dependence on plasma parameters, for example on the density gradient length. The pinch leads to an increase of the inward flux of momentum with increasing toroidal rotation. There is indeed a hint of this in the JET database, showing the effective Prandtl number to decrease as a function of increasing Mach number, although in principle it is not guaranteed that the lowering of the effective Pr number is necessarily representing an increase of pinch, but rather a relative change in momentum and ion heat diffusivities (figure not shown here due to space limitations).

For the JET Pulse No. 66128 (momentum modulation experiment studied in section 3), LINART predicts $\chi_\phi/\chi_i = 1.01$ and a pinch number of $Rv_{pinch}/\chi_\phi = -2.3$. The pinch number is calculated by using the input data from JET Pulse No. 66128, and by scanning the normalised toroidal velocity gradient u' to zero. The full scan from LINART is presented in figure 4 (red line) where the momentum flux normalised with the ion heat flux is plotted as a function of u'. The value of the pinch can be inferred from the value on the y-axis at $u' = 0$. The slope of the curve indicates the Prandtl number. The same quantities can be calculated from the experiment and are shown in blue. Note that the experiments are done for one set of parameters and, therefore, only one point as well as the slope of the curve in that point can be given in Fig.4. The experimental pinch $Rv_{pinch}/\chi_\phi \approx -5$ is somewhat larger than that of LINART. The predicted and experimental Prandtl numbers are in excellent agreement, thus yielding parallel but shifted lines in figure 4.

Three other experimental pulses, one low density *H*-mode (Pulse No. 59217), one medium density hybrid (Pulse No. 60931) and one high density *H*-mode (Pulse No. 57865) have been modelled both with LINART as well as with the non-linear global gyro-kinetic code GYRO [36]. For all shots, LINART predicts significant momentum pinch, and the effective Prandtl numbers from LINART and experiment are in fairly good agreement. First simulations using GYRO predicts Prandtl numbers between $\chi_{\phi,eff}/\chi_{i,eff}$=0.8–1, higher than the experiments which are yielded values around $\chi_{\phi,eff}/\chi_{i,eff}$=0.2–0.4. At present the reason for this discrepancy is unclear. However, it is known that non-linear with GYRO are very sensitive to the input plasma profiles. It is to be noted that a previous benchmark between LINART and GYRO yielded good agreement and that the profiles in the simulations are not exactly the same due to the different set up of the codes. Also the effect of the $E\times B$ shear on the momentum transport [37, 38, 39] is absent in LINART but included in GYRO. Finally, there is some evidence for a momentum flux driven by the density and temperature gradients in global simulations [40], although the magnitude is expected to be small.

An extensive transport modelling study has also been performed for high and low density ELMy *H*-mode discharges, hybrid scenario discharges and *L*-mode discharges. A new version of the Weiland model that includes self-consistent treatment of the toroidal velocity has been developed [41]. In addition, momentum transport has been modelled with GLF23 transport model [17, 42]. A comparison of the simulated toroidal velocity and ion and electron temperatures with experimental data gives typically around 15% Root-Mean-Square (RMS) error between the simulated and experimental data, both models being roughly as accurate [43,9]. In particular, the RMS error for toroidal velocity is of the same order as that of the temperatures. Interestingly, the models are most

accurate to predict $\ldots_f$ in the high density plasmas where the effective Prandtl number is small and the ITG is the dominant micro-instability. The good agreement of these model predictions of $\ldots_f$ with the experiment is based on the low predicted Prandtl number $«_f/«_i$ since the pinch in these models is small to the extent that the diffusive and pinch terms can be separated in the model. In order to fully test the capability of the fluid transport models to predict momentum transport, the modulation experiments must be modelled, a task left for future work.

5. ANOMALOUS POLOIDAL VELOCITY AND ITS RELATION TO THE DYNAMICS OF THE ITBS

The physics of flows in the poloidal direction is quite different from those in the toroidal direction where the toroidal symmetry plays a strong role. The poloidal velocity is strongly damped, roughly within the ion-ion collision time, due to the lack of poloidal symmetry in a tokamak. Consequently, the poloidal velocity is usually assumed to be described well by the neo-classical transport theory [44]. However, recently both DIII-D [15] and JET [14] have reported measurements on anomalous poloidal velocity v_θ, being an order of magnitude larger than the neo-classical estimate from the neo-classical transport code NCLASS [45]. On JET, a spin-up of v_θ within the ITB is observed. The measured carbon v_θ can be an order of magnitude larger within the ITB than its neo-classical estimate and even the sign of the measured carbon v_θ can be different from the neo-classical one in some radial regions, and furthermore, can change sign within the ITB.

Due to the large difference in v_θ between the measured value and the neo-classical estimate, the evaluated radial electric field E_r from equation (1) depends thus on the source of v_θ and is in most cases much larger when the measured v_q is used instead of the neo-classical one. In particular, even if the absolute value of E_r is not always larger when using the measured v_θ, the $E\times B$ flow shear within the fully developed ITB certainly is significantly larger. This is particularly interesting for transport simulations where predicting the dynamics of the ITBs has turned out to be extremely challenging [46]. There are most probably several reasons for having difficulties predicting ITBs, but one of the reasons, not taken into account earlier is that past transport simulations have always assumed that the poloidal rotation velocity is neo-classical. Therefore, the used $E\times B$ flow shear in the transport simulations has not been appropriate. Using the experimental v_θ instead of the neo-classical, both the Weiland transport model and GLF23 are able to form the ITB roughly at the experimental location [9]. Otherwise identical simulations except with v_θ from NCLASS instead of the experimental one does not exhibit any sign of an ITB in either case. However, in order to genuinely improve our predictive capabilities, one should also be able to predict the increase in v_θ self-consistently rather than using the experimentally measured data. This work is on-going and the Weiland model has been upgraded to include an equation for v_θ that allows self-consistent simulations of ITBs and poloidal velocity evolution for the first time within a transport model. The first simulation results with the model show that the model predicts v_θ spin-up within the ITB in qualitative agreement with experiment.

One of the most interesting issues with the spin-up of v_θ in connection with ITBs is the question of causality, i.e. whether the ITB is triggered before or after the spin-up of v_θ. Experimental evidence so far indicate that the ITB and v_θ form and grow simultaneously while the role of v_θ in the preceding ITB triggering event is still unclarified. The predictive simulations with the Weiland model with self-consistent modelling of v_θ also show that during the phase where the ITB is formed, the ITB grows together with the simultaneous increase of v_θ. And again, there is no evidence in the simulation that v_θ has had a special role in the preceding ITB triggering event before the dynamical formation/ grow phase. Thus, no clear sequence of causality has been observed either in the experiments or in transport modelling. The source for the predicted high v_θ is the turbulent flow generation through the Reynold's stress where trapped particles play a key role. In standard ELMy H-mode plasmas the model does not predict any flow generation significantly above the neo-classcial level.

Another key point related to the observed spin-up of v_θ is to understand what mechanism drives its value to such high values, much larger than the standard neo-classical theory predicts. On JET, the generation of the poloidal flow has been studied with three different turbulence codes; with the electro-static TRB turbulence code [47] that solves fluid equations for ITG/TEM turbulence, with non-linear 3D global electromagnetic fluid turbulence code CUTIE [48] and with non-linear 3D global electromagnetic fluid turbulence code GEM [49]. TRB and CUTIE results that have already been reported in detail in Ref. [9], both codes find a strong drive of v_θ from the Reynold's stress around the radial location of the ITB. This drive is able to overcome the neo-classical damping, predicting thus velocities higher than the neo-classical estimate from NCLASS code. However in TRB, the m=1, n=0 components are not calculated explicitly. As a consequence the physics of Geodesic Acoustic Modes (GAMs) is not covered in these simulations, while they are known to influence the momentum balance equation [49,50,51]. On the other hand, in CUTIE the treatment of equilibrium is simplified and the trapped particle physics neglected. In particular the treatment of the equilibrium is known to influence significantly the poloidal velocities calculated in the code and affects the role of GAMs. Consequently, the results should be considered as indicative, and most probably provide an upper bound of the mean poloidal velocity as results from other codes including GAM dynamics show that they often serve as a damping mechanism to flows [49,50].

The neo-classical equilibrium is calculated
more accurately in the GEM code, and the preliminary results from the simulations suggest that the spin-up of v_θ is a consequence of the plasma profiles steepening when the ITB grows. The spin-up of v_θ follows in particular the growth of the toroidal velocity within the ITB as v_θ and v_ϕ are tight together via the radial force balance in equation (1). However, the neo-classical equilibrium calculation with GEM allows the predicted v_θ to deviate from v_θ calculated with standard neo-classical tools like NCLASS. This result would in principle be able to solve the question of causality, with v_θ spin-up being a consequence of the ITB, in particular in the phase where the ITB is forming and growing. However, these simulation results do not exclude any role that v_θ or time-varying zonal flows might have had in the initial trigger phase of the ITB. The GEM results also suggest

that the present neo-classical transport codes may not solve the neo-classical equilibrium (in particular in 2D) with very strong flows in an accurate enough way. In any case, more work is needed both on the experimental front and modelling side to solve the causality question and fully understand the reason for the spin-up of v_θ within the ITB.

CONCLUSIONS

We conclude the paper by addressing the issues raised in the introduction. Momentum and heat transport are clearly related in tokamaks, the global energy and momentum times being very similar among many devices. The local transport studies in the core plasma are more scattered with respect to the effective Prandtl number among the tokamaks, being very low around 0.2 for example on JET. The difference is not understood for the time being, could be for example due to magnitude of inward pinch varying from tokamak to tokamak. Experimental evidence on JET and JT-60U show that the Prandtl number based on diffusive terms only should, however, be close to 1, combined with a significant inward pinch velocity, resulting in a low effective Prandtl number. The experimental results, i.e. the Prandtl number around 1 and large pinch, are in good qualitative and to some extent also in quantitative agreement with linear gyro-kinetic simulations. Concerning the predictions in ITER, understanding of core momentum transport has increased very remarkably thanks to the recent perturbative momentum transport experiments and recent development in gyro-kinetic and fluid theory including momentum transport. In addition, rotation has been studied intensively in plasmas without NBI torque in many tokamaks recently. However, to predict the full radial rotation profile, the momentum pedestal must be known, and the characteristic of momentum transport in the plasma edge and pedestal are much less studied. In particular, the role of toroidal magnetic field ripple as a source of torque is very important at the level of ripple in ITER. However, experimental results from JET and JT-60U have been reported recently and code development is on-going. Consequently, in the near future we expect to be able to make a first reasonably founded prediction of the toroidal momentum profile in ITER.

Poloidal velocity is not always in agreement with the neo-classical estimate in tokamaks. On JET, the spin-up of v_θ occurs simultaneously with the growth of the ITB, thus the causality not being resolved in experiments. The Weiland model also predicts similar chain of causality in self-consistent transport simulations of the ITB and v_θ i.e. they form and grow hand-in-hand. Concerning the drive of v_θ spin-up, the fluid turbulence simulations with CUTIE and TRB using a simplified equilibrium treatment, and also transport simulations with the Weiland model as well show the strong turbulent drive of v_θ from the Reynold's stress. On the other hand, another explanation for v_θ spin-up is suggested by the GEM fluid turbulence code with detailed neo-classical equilibrium treatment. It shows that v_θ is a consequence of the plasma profiles within the ITB, in particular that of v_ϕ, suggesting that the observed spin-up of v_θ within the ITB is a consequence rather than a cause of the ITB. More work is needed both on the experimental front and modelling side to solve the causality question and fully understand the reason for the spin-up of the v_θ within the ITB.

REFERENCES

[1]. Biglari H., Diamond P.H. and Terry P.W. 1990 *Phys. Fluids B* **2** 1.

[2]. R.L Miller and Waltz R.E. *et al*. 1994 Phys. *Plasmas* **1** 2835.

[3]. Burrell K.H. 1997 *Phys. Plasmas* **4** 1499.

[4]. Garofalo A.M. *et al*. 2001 Nucl. *Fusion* **41** 1171.

[5]. Liu Y. *et al*. 2005 *Nucl. Fusion* **45** 1131.

[6]. Liu Y. *et al*. 2006 *Phys. Plasmas* **13** 056120.

[7]. Reimerdes H. et al. 2006 Phys. Plasmas **13** 056107.

[8]. de Vries P.C. et al. 2006 Plasma Phys. Control. Fusion **48** 1693.

[9]. Tala T. *et al*. 2007 "Toroidal and poloidal momentum transport on JET", accepted for publication in Nucl. Fusion.

[10]. Nishijima *et al*. 2005 *Plasma Phys. Control. Fusion* **47** 89.

[11]. Peeters A.G. and Angioni C. 2005 *Phys. Plasmas* **12** 072515.

[12]. Strintzi D. and Peeters A.G. 2007 ´†Influence of kinetic electrons on the toroidal momentum diffusivity in a tokamak plasma", submitted to Phys. Plasmas.

[13]. Peeters A.G., C. Angioni, D. Strintzi 2007 *Phys. Rev. Lett*. **98** 265003.

[14]. CrombÈ K. *et al*. 2005 *Phys. Rev. Lett*. **95** 155003.

[15]. Solomon W.M. *et al*. 2006 *Phys. Plasmas* **13** 056116.

[16]. Bell R.E. *et al*. 1998 *Phys. Rev. Lett*. **81** 1429.

[17]. Waltz R.E. *et al*. 1997 *Phys. Plasmas* **4** 2482.

[18]. Zastrow K.-D. *et al*. 1998 *Nucl. Fusion* **38**†257.

[19]. Kallenbach A. *et al*. 1991 *Plasma Phys. Control. Fusion* **33**†595.

[20]. de Grassie J.S. *et al*. 2003 *Nucl. Fusion* **43**†142.

[21]. Scott S.D. *et al*. 1990 *Phys. Rev. Lett*. **64**†531.

[22]. Asakura A. *et al*.1993 *Nucl. Fusion* **33** 1165.

[23]. Rice J.E. *et al*. 2004 *Phys. Plasmas* **11** 2427.

[24]. deGrassie J.S. *et al*. 2004 *Phys. Plasmas* **11** 4323.

[25]. Bortolon A. *et al*. 2006 Phys. Rev. Lett. **97** 235003.

[26]. L.-G. Eriksson *et al*., "Toroidal Rotation in RF Heated JET Plasmas", *Proc. in RF in 17th Topical Conf on Radio Frequency Power in Plasmas, Clearwater, Florida, USA, May 7-9, 2007*.

[27]. Nave F. *et al*. 2007 Proc. 32nd European Physical Society Conf. on Control. Fusion and Plasma Phys. (Warsow, Poland, 2 July - 6 July 2007).

[28]. Rice J. *et al*. 2006 *Proc. 21st Fusion Energy Conference (Chengdu, China, 16 – 21 October 2006) Paper EX/P3-12*.

[29]. Mattor N. and Diamond P.H. 1988 *Phys. Fluids* **31** 1180.

[30]. Angioni *et al*. 2006 *Proc. 21st Fusion Energy Conference (Chengdu, China, 16 – 21 October 2006) Paper EX/8-5Rb*.

[31]. Yoshida M. *et al*. 2007 Momentum Transport and Plasma Rotation Profile in Toroidal Direction in JT-60U L-mode plasmas accepted for publication in *Nucl*. *Fusion*.
[32]. Scott S.D. *et al*. 1990 *Phys*. *Fluids B* **2** 1300.
[33]. Hahm T.S. *et al*. 2007 "Nonlinear Gyrokinetic Theory of Toroidal Momentum Pinch", *submitted to Phys*. *Plasmas*.
[34]. Genacchi G. and Taroni A. 1988 *JETTO: A free boundary plasma transport code (basic version) Rapporto ENEA RT/TIB 1988(5)*.
[35]. Peeters A.G. and Strintzi D. 2004 *Phys*. *Plasmas* **11** 3748.
[36]. Candy J. and Waltz R.E. 2003 *Phys*. *Rev*. *Lett*. **91** 045001.
[37]. Dominguez R.R. and Staebler G.M. 1993 *Phys*. *Fluids B* **5** 3876.
[38]. Garbet X. *et al*. 2002 *Phys*. *Plasmas* **9** 3893.
[39]. Gürcan Ö.D. *et al*.2007 Phys. Plasmas **14** 042306.
[40]. Peeters A.G. *et al*. 2006 *Plasma Phys*. *Control*. *Fusion* **48** B413.
[41]. Weiland J. and Nordman H. 2006 *Proc*. *33rd European Physical Society Conf*. *on Control*. *Fusion and Plasma Phys*. *(Rome, Italy, 19-23 June 2006) ECA* **30** P2.186.
[42]. Kinsey J.E., Staebler G.M. and Waltz R.E. 2005 *Phys*. *Plasmas* **12** 052503.
[43]. Eriksson A. *et al*. 2007 Predictive simulations of toroidal momentum transport at JET, to be submitted to Plasma Phys.Control. Fusion.
[44]. Hirshman S.P. and Sigmar D.J. 1981 *Nucl*. *Fusion* **21** 1079.
[45]. Houlberg W. *et al*. 1997 *Phys*. *Plasmas* **4** 3231.
[46]. Tala T. *et al*. 2006 *Nucl Fusion* **46**†548.
[47]. Garbet X. and Waltz R.E. 1996 *Phys*. *Plasmas* **3**1898.
[48] . Thyagaraja A. *et al*. 2005 *Phys*. *Plasmas* **12** 090907.
[49]. Scott B.D. 2006 *Plasma Phys*. *Control*. *Fusion* **48** B277.
[50]. Naulin V. *et al*. 2005 *Phys*. *Plasmas* **12** 052515.
[51]. Miyamoto N. *et al*. 2004 *Phys*. *Plasmas* **11** 5557.

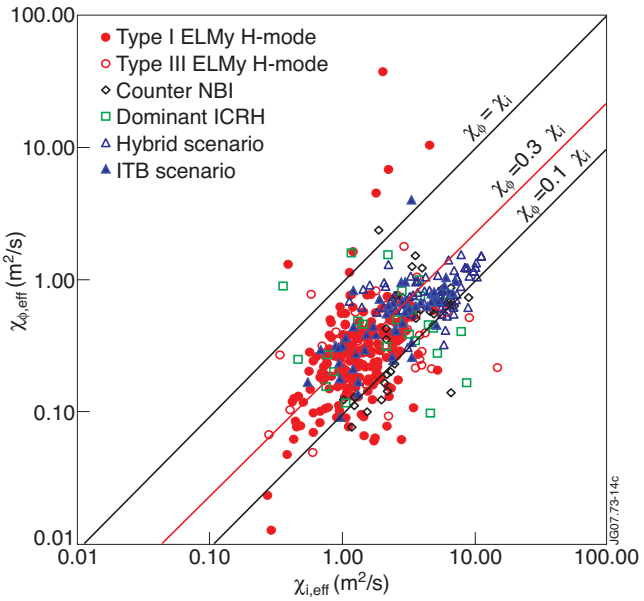

Figure 1. Effective momentum diffusivity versus effective ion heat diffusivity for large number of discharges from the JET momentum database, covering plasmas from several different plasma operating scenarios.

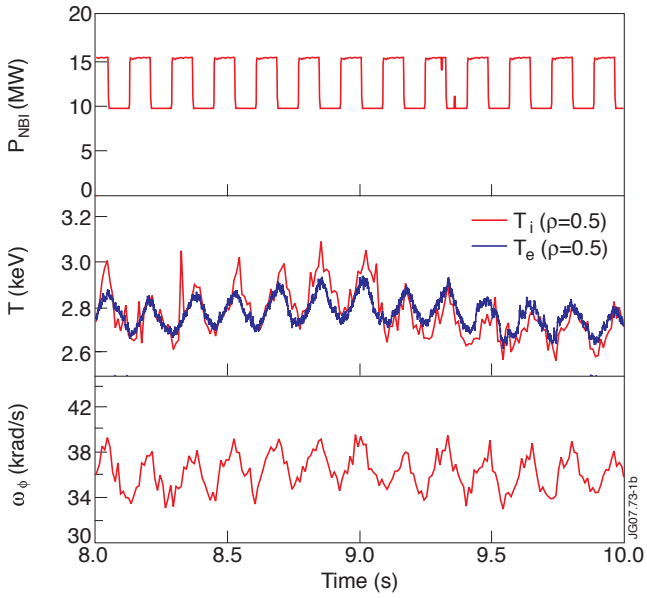

Figure 2. NBI power, ion and electron temperatures and toroidal angular frequency ω_ϕ. zoomed into the middle of the modulation phase for JET Pulse No. 66128.

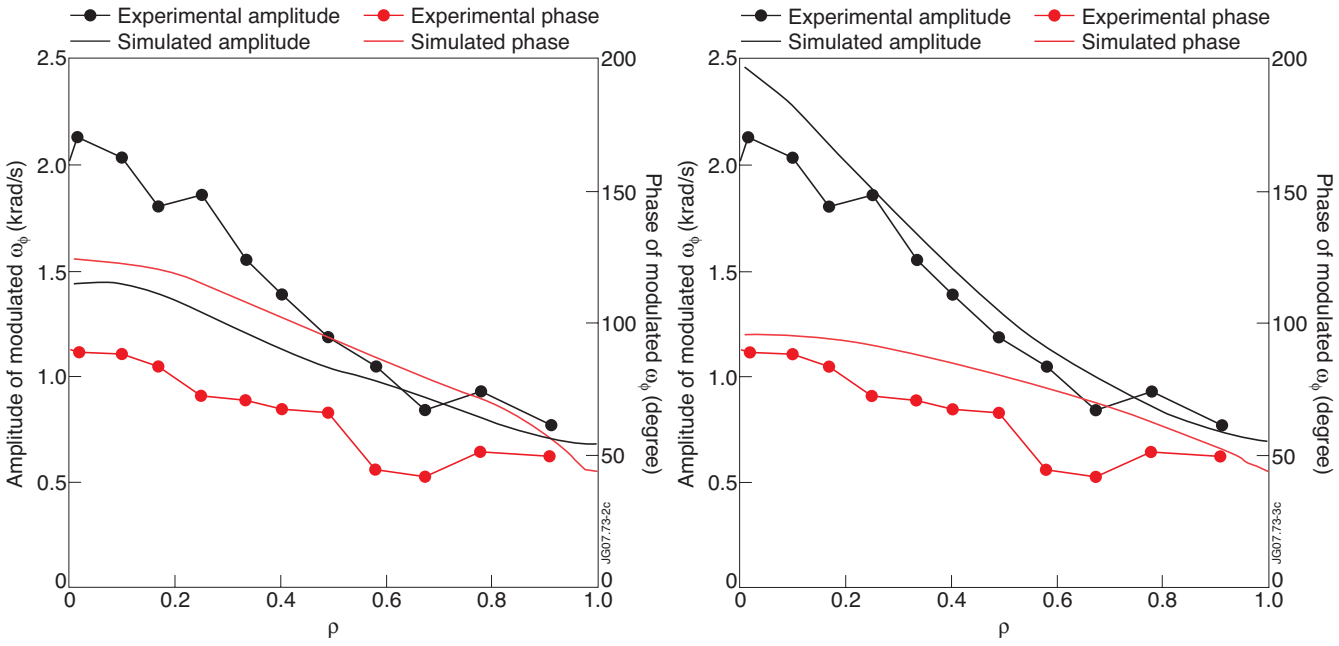

Figure 3. Comparison of the experimental (lines with dots) and simulated (lines) amplitudes (black) and phases (red) of modulated ω_ϕ with the simulation choices χ_f/χ_i=0.25 and v_{pinch} = 0 (left frame) and χ_f/χ_i=1.0 and v_{pinch}=15m/s (right frame) for JET pulse no. 66128.

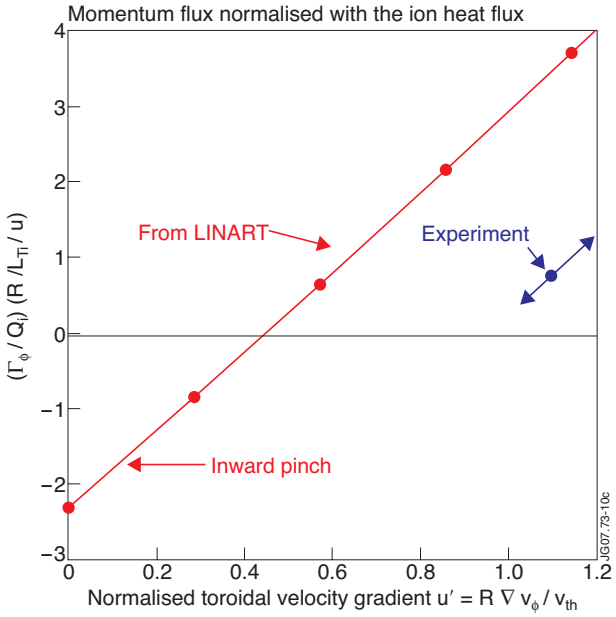

Figure 4. Momentum flux normalised to the ion heat flux as function of normalised toroidal velocity gradient for LINART gyro-kinetic simulations (red curve) and experiment (blue point with arrows indicating the inferred Prandtl number) for JET Pulse No 66128.